Extended Abstracts of the 2006 International Conference on Solid State Devices and Materials, Yokohama, 2006, pp. 982-983

F-7-1 The incorporation effect of thin Al_2O_3 layers on ZrO_2-Al_2O_3 nanolaminates in the composite oxide-high-K-oxide stack for the floating gate flash memory devices

Moon Sig Joo,* Seung Ryong Lee, Hongseon Yang, Kwon Hong, Se-Aug Jang, Jaehyoung Koo, Jaemun Kim, Seungwoo Shin, Myungok Kim, Seungho Pyi, Nojung Kwak, and Jin-Woong Kim

R&D Division, Hynix Semiconductor Inc., San 136-1, Ami-ri, Bubal-eub, Icheon-si, Kyoungki-do 467-701, Korea,

Phone: 82-31-630-5288, Fax: 82-31-630-4545, *email: *moonsig.joo@hynix.com*

Introduction

Aggressive scaling of flash memory devices requires the inter-poly dielectrics (IPD) layer with high-K dielectric to enhance the coupling ratio [1-3]. However, most of high-K dielectrics except Al_2O_3 tend to be crystallized during deposition or subsequent thermal processes, forming grain boundaries which serve as leakage current paths and impurity diffusion paths [4-6]. Therefore, like HfAlO film for gate dielectric application, the incorporation of Al_2O_3 into high-K dielectric is needed to improve the leakage current characteristics and retard the impurity diffusion through the film [7,8]. In this paper, we fabricate ZrO_2-Al_2O_3 nanolaminates and present the effect of Al_2O_3 incorporation on their electrical properties and reliabilities in the composite oxide-high-K-oxide (OKO) stack.

Experimental

Double polysilicon planar-type capacitors were fabricated using in-situ phosphorous-doped polysilicon for control and floating gates on thick thermal oxides. Between two gate electrodes, OKO stack consisting of about 52-Å-thick bottom oxide, high-K dielectric stack, and 42-Å-thick top oxide was fabricated. Three kinds of ZrO_2-Al_2O_3 nanolaminates as high-K dielectric stacks were deposited by Atomic Layer Deposition (ALD) as shown in Table 1; ZAZ, AZAZA, and AZAZAZA stack. The total thickness of each nanolaminate with Al_2O_3 film of around 4 Å was designed to be around 44 Å. For comparison, pure ZrO_2 and Al_2O_3 samples were also prepared by ALD. After patterning the capacitors, all samples were subjected to the polysilicon anneal in a N_2 ambient at 920ºC for 20 minutes.

Results and discussion

The thermal stability of the ZAZ stack is investigated using HRTEM as shown in Fig. 1. As-deposited ZAZ stack shows an amorphous structure and clear boundaries between ZrO_2 and about 4-Å-thick Al_2O_3 layer. After subsequent thermal processes, it is interesting to note that some amorphous regions exist embedded in the crystallized high-K film, probably due to the higher crystallization temperature of Al_2O_3 film compared to ZrO_2 film. It indicates that the Al_2O_3 layer might lead to the mismatch of grain boundaries between polycrystalline ZrO_2 layers, which may reduce the leakage current path and impurity diffusion path along the grain boundaries.

Figure 2 shows the capacitive equivalent thickness (CET) as a function of mole fraction of Al_2O_3 in the ZrO_2-Al_2O_3 stacks. Unlike the previous work,[10] the CET value of the ZrO_2-Al_2O_3 stacks decreases as the fraction of Al_2O_3 increases until 36 %. It is worth to note that although ZrO_2 layers with higher permittivity are substituted with Al_2O_3 capping layers with lower permittivity, the CET values of AZAZA do not increase but even decrease by around 3 Å compared to the ZAZ stack. It can be explained by the silicon incorporation effect into the ZAZ stack during top oxide deposition and/or subsequent thermal processes. The silicon atoms that diffuse through upper ZrO_2 film stop at the Al_2O_3 inserting layer of the ZAZ stack and form Zr-silicate there, causing the reduction of the overall dielectric constant of the nanolaminate. The formation of Zr-silicate is confirmed by X-ray Photoelectron Spectroscopy (XPS) analysis as shown in Fig. 3. However, for AZAZA and AZAZAZA stacks, the Al_2O_3 capping layers can reduce the silicon diffusion into ZrO_2 film due to much enhanced resistance to impurity diffusion, resulting in less reduction of the overall dielectric constant of the stacks.

The leakage current characteristics of OKO stacks are investigated through a plot of leakage-current versus CET as shown in Fig. 4. As a reference, those of Al_2O_3 films in OKO stack are used. ZrO_2 film shows little improvement of leakage currents for both side injections compared to Al_2O_3 film at the same CET, whereas the ZAZ stack shows much improved leakage current characteristics, especially under control gate side injection. These improvements are mainly attributed to the reduction of the leakage current paths by mismatch of grain boundaries of polycrystalline ZrO_2 films as discussed in Fig. 1. Further improvements are observed in AZAZA and AZAZAZA stacks for both side injections. These improvements are possibly due to the CET reduction by the enhanced resistance to silicon diffusion by Al_2O_3 capping layers as discussed in Fig. 2.

Figure 5 shows the Weibull plots of ZrO_2 and ZrO_2-Al_2O_3 stacks as a function of the time-to-breakdown (T_{bd}) measured at the constant voltage stress and under both polarity injections. For positive polarity stress, ZAZ and AZAZA stacks show improved breakdown characteristics compared to the ZrO_2 film, probably due to the thicker CET's of ZAZ and AZAZA stacks than that of ZrO_2. On the other hand, for negative polarity stress, ZAZ and AZAZA stacks show a substantial improvement compared to the ZrO_2 film that shows nearly initial breakdown characteristics. This improvement is mainly due to the enhanced immunity to more energetic electron of ZAZ and AZAZA stacks, which can be explained by the increase in the energetic-electron hardness by Al_2O_3 inserting layer [9]. However, AZAZAZA stack also shows same trend with ZrO_2 film. The degradation for AZAZAZA is probably attributed to the disappearance of the Al_2O_3 inserting layers by the formation of Zr-aluminate by intermixing of Al_2O_3 and ZrO_2 during subsequent thermal processes because each ZrO_2 film of about 9 Å between Al_2O_3 layers is too thin, which is confirmed by HRTEM as shown in Fig. 6.

Conclusions

We demonstrate the incorporation effects of thin Al_2O_3 layers into ZrO_2 films on electrical properties and reliability in the composite OKO stack for floating gate flash memory devices. The optimized ZrO_2-Al_2O_3 nanolaminate shows the significantly improved leakage-current versus CET and TDDB characteristics compared to the pure ZrO_2 owing to the mismatch of grain boundaries, the improved resistance to silicon diffusion through ZrO_2 layer, and the enhanced energetic-electron hardness of the film by the incorporation of Al_2O_3 layers.

References

[1] K. Kim, IEDM Tech. Digest, 13.5, 2005.
[2] T.-P. Lee, et al, J. Vac. Sci. Technol. B 22, p. 2295, 2004.
[3] M. V. Duuren, et al., Proc. NVSMW, p. 52, 2006.
[4] C.H. Choi, et al, IEDM Tech. Digest, p. 857, 2002.
[5] M.S. Joo, et al, IEEE T-ED, 50, p. 2088, 2003.
[6] H.Y. Yu, et al, Appl. Phys. Lett., 81, p. 3618, 2002.
[7] D.C. Gilmer, et al, Appl. Phys. Lett., 81, p. 1288, 2002.
[8] L. Manchanda, et al, Microelectronic Engineering, 59, p. 351, 2001.
[9] T. Yamaguchi, et al, Proc. IRPS, 34, p. 34, 2003.

Table 1. The structure of ZrO_2 and ZrO_2-Al_2O_3 nanolaminates.

Stack	Structure	Thickness (Å)
ZrO_2	ZrO_2	44
ZAZ	$ZrO_2/Al_2O_3/ZrO_2$	20/4/20
AZAZA	$Al_2O_3/ZrO_2/Al_2O_3/ZrO_2/Al_2O_3$	4/16/4/16/4
AZAZAZA	$Al_2O_3/ZrO_2/Al_2O_3/ZrO_2/Al_2O_3/ZrO_2/Al_2O_3$	4/9/4/10/4/9/4

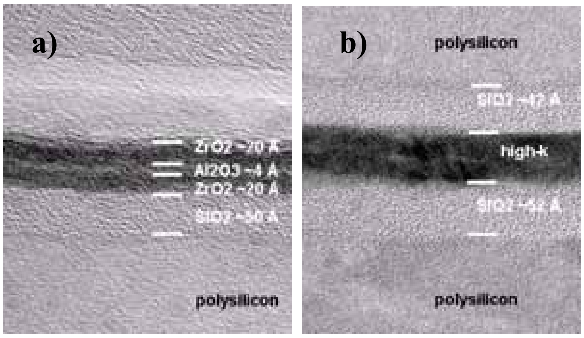

Fig. 1. (a) HRTEM images of as-deposited ZAZ stack on the bottom oxide and floating gate polysilicon. (b) HRTEM images of the ZAZ stack in the composite oxide-high-K-oxide stack after subsequent thermal processes. There exist some amorphous regions embedded in the crystallized ZrO_2 film.

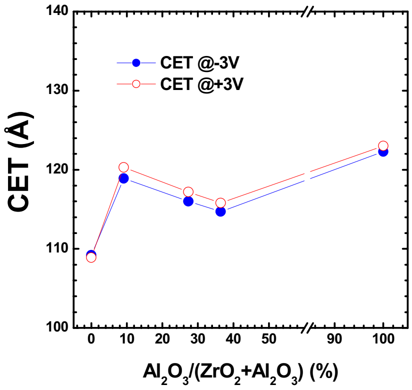

Fig. 2. The CET as a function of mole fraction of Al_2O_3 in the ZrO_2-Al_2O_3 nanolaminates at the almost same physical thickness of 44 Å. The CET values of each sample were obtained from the capacitance values at gate biases of ± 3V at 100 kHz frequency and compared to those of pure ZrO_2 and Al_2O_3 films.

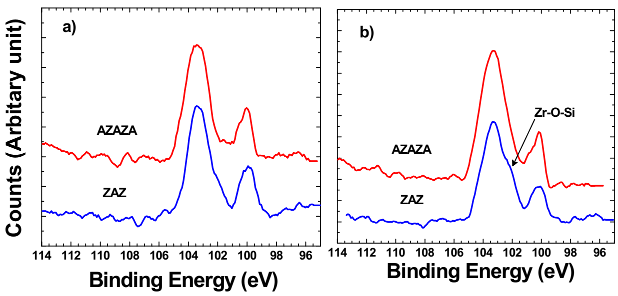

Fig. 3. Si2p core-level spectra of ZAZ and AZAZA stacks (a) before and (b) after top oxide deposition. After top oxide deposition in SiH_2Cl_2 and N_2O ambient, the ZAZ stack show a shoulder at around 102.0 eV, which indicates Zr silicate bond (Zr-O-Si) formation.

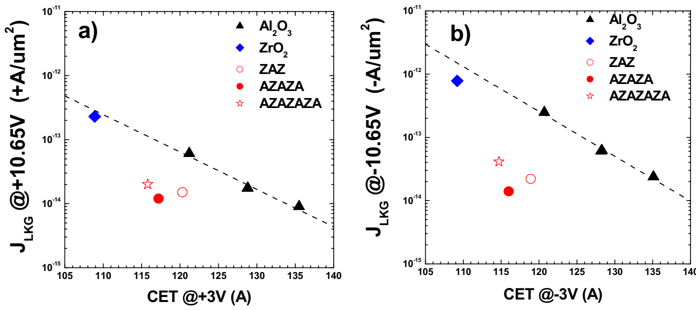

Fig. 4. The leakage current (J_{LKG}) characteristics of OKO stacks in the plot of J_{LKG} versus CET under (a) floating gate side injection (b) control gate side injection. All the ZrO_2-Al_2O_3 nanolaminates show much improved leakage currents characteristics compared to the Al_2O_3 film at the same CET, especially under control gate side injection.

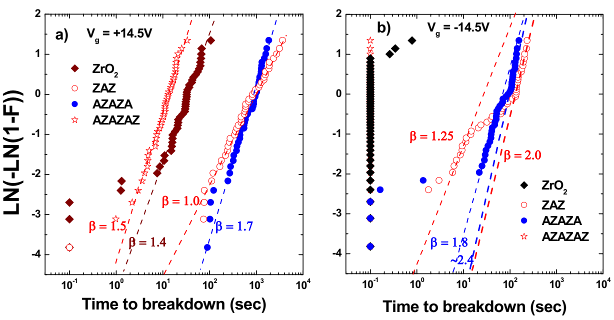

Fig. 5. The Weibull plots of ZrO_2 and ZrO_2-Al_2O_3 stacks as a function of the time-to-breakdown (T_{bd}) measured at the constant voltage stress and under (a) positive polarity stress and (b) negative polarity stress. The stress voltages are +14.5 V and -14.5 V, respectively. The ZAZ stack seems to have the T_{bd} distribution with the bi-modal breakdown process under negative polarity stress, having small (with β=1.25) and large (with β=2.0) T_{bd} distribution components together.

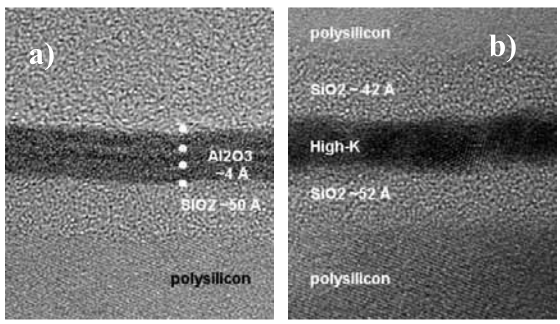

Fig. 6. (a) HRTEM images of as-deposited AZAZAZA stack on the bottom oxide and floating gate polysilicon. It also shows an amorphous structure and boundaries between ZrO_2 and Al_2O_3 layer. (b) HRTEM images of the AZAZAZA after subsequent thermal processes. All the layers are mixed after subsequent thermal processes.